

## Electron Spin Resonance in Nickel-Doped Germanium

G. W. LUDWIG AND H. H. WOODBURY  
*General Electric Research Laboratory, Schenectady, New York*  
 (Received October 10, 1958)

Electron spin resonance absorption proportional in intensity to the  $\text{Ni}^-$  concentration has been detected at 14 kMc/sec in germanium crystals. The spectrum, which consists of six main lines having anisotropic  $g$  values, is interpreted in terms of a Jahn-Teller distortion of the nickel ion in any cubic direction. The principal axes of the  $g$  tensor are the cubic direction and two mutually perpendicular  $[110]$  directions having  $g$  values of 2.0294, 2.0176, and 2.1128, respectively. Hyperfine structure due to  $\text{Ni}^{61}$  in enriched samples shows the same principal axes and principal values of  $\leq 1.6$ , 12.2, and 10.3, respectively, in units of  $10^{-4} \text{ cm}^{-1}$ , and establishes the spin of that isotope as  $\frac{3}{2}$ . Hyperfine interaction with  $\text{Ge}^{73}$  in the two nearest neighbor positions toward which the nickel atom moves in the Jahn-Teller distortion has been resolved and ranges from  $19.8 \times 10^{-4} \text{ cm}^{-1}$  for the magnetic field in the  $\text{Ni-Ge}^{73}$  direction to  $16.5 \times 10^{-4} \text{ cm}^{-1}$  at right angles to this axis. Above  $20.4^\circ\text{K}$  the Jahn-Teller distortion reorients with increasing rapidity. The line broadening and eventual merging has been studied and estimates have been made of the activation energies for reorientation by inversion and by rotation.

### INTRODUCTION

NICKEL introduced as an impurity into germanium shows two acceptor levels, one 0.22 eV from the valence band and one 0.30 eV from the conduction band.<sup>1</sup> Crystals containing  $7 \times 10^{15} \text{ Ni/cm}^3$  introduced by diffusion<sup>2</sup> at  $850^\circ\text{C}$  were examined by spin resonance methods. The filling of the two acceptor levels was controlled by the amount of arsenic introduced into the germanium crystals at the time they were pulled from the melt. Spin resonance absorption<sup>3</sup> was detected proportional to the percentage of the lower acceptor level which was filled. It decreased, however, proportional to the percentage of the upper acceptor level which was filled. These observations further confirm the double-acceptor model for nickel, according to which both acceptor levels are associated with the same impurity site. When both levels are empty or full, the nickel is in the form  $\text{Ni}^0$  or  $\text{Ni}^-$ , respectively. If only the lower level is full, the nickel is in the form  $\text{Ni}^-$ , which is the charge state for which spin resonance absorption is detected.

Spin resonance measurements on nickel in the form  $\text{Ni}^{++}$  have been reported in the literature for a number of compounds.<sup>4</sup> In these compounds an orbital singlet lies lowest, the configuration is  $3d^8$ , and the effective spin equals the actual spin ( $S=1$ ). The  $g$  tensor is nearly isotropic, and no hyperfine structure due to the isotope  $\text{Ni}^{61}$  (natural abundance 1.25%) has been reported. Nickel in germanium thus represents the first case for which resonance due to  $\text{Ni}^-$  (with an effective spin  $\frac{1}{2}$ ) has been observed, and also the first case in which the hyperfine interaction with  $\text{Ni}^{61}$  has been detected.<sup>5</sup>

<sup>1</sup> Tyler, Newman, and Woodbury, *Phys. Rev.* **98**, 461 (1955).  
<sup>2</sup> W. W. Tyler and H. H. Woodbury, *Bull. Am. Phys. Soc. Ser. II*, **2**, 135 (1957). A more complete discussion will be published.  
<sup>3</sup> G. W. Ludwig and H. H. Woodbury, *Bull. Am. Phys. Soc. Ser. II*, **3**, 135 (1958).  
<sup>4</sup> K. D. Bowers and J. Owen, in *Reports on Progress in Physics* (The Physical Society, London, 1955), Vol. 18, p. 304; W. Low, *Phys. Rev.* **101**, 1827 (1956).  
<sup>5</sup> H. H. Woodbury and G. W. Ludwig, *Phys. Rev. Letters* **1**, 16 (1958).

$\text{Mn}^-$  is the only other impurity in germanium for which spin resonance information appears in the literature.<sup>6</sup>

### EQUIPMENT

A balanced bolometer homodyne detection system is used. A Varian VA92-C klystron, stabilized on an external cavity using a Pound dc stabilization scheme, is the microwave source. A Varian V-4012-3B magnet, which can be rotated in a horizontal plane, is scanned in field to detect resonance. The sample is contained in a  $TE_{011}$  mode reflection cavity overcoupled to minimize FM noise when the spectrometer is tuned to absorption.<sup>7</sup> The brass construction of the cavity permits penetration of the audio-frequency modulation of the magnetic field and results in nearly constant cavity  $Q$  and coupling coefficient as a function of temperature. The cavity terminates one arm of a magic tee bridge, which is normally operated at balance. The signal power from the bridge goes to another magic tee, the detection tee, where it is split to feed two bolometers. These bolometers are biased with power fed through the fourth arm of the

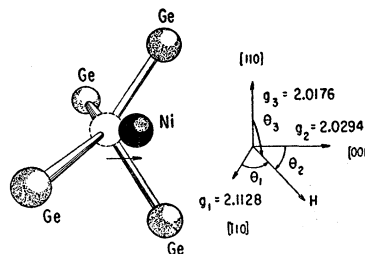


FIG. 1. Model for the  $\text{Ni}^-$  site in the germanium lattice. Due to the Jahn-Teller distortion the nickel atom moves from the substitutional site in a cubic direction (e.g., toward the position of the black ball).  $g = (g_1^2 \cos^2 \theta_1 + g_2^2 \cos^2 \theta_2 + g_3^2 \cos^2 \theta_3)^{1/2}$ , where  $g_1, g_2, g_3$  are the principal values of the  $g$  tensor, and  $\theta_1, \theta_2, \theta_3$  are the angles between the magnetic field and the principal axes of the  $g$  tensor.

<sup>6</sup> G. D. Watkins, *Bull. Am. Phys. Soc. Ser. II*, **2**, 345 (1957).  
<sup>7</sup> G. Feher, *Bell System Tech. J.* **36**, 449 (1957).

detection tee. A phase shifter in the fourth arm allows adjustment of the phase of the bias voltage relative to that of the signal voltage making the system sensitive to the real part  $\chi'$  or the imaginary part  $\chi''$  of the magnetic susceptibility of the sample as desired. In operation, up to 40 mw of microwave power at approximately 14 kMc/sec is incident on the sample cavity. The klystron frequency is measured with a Hewlett-Packard 540 A Transfer Oscillator and a Hewlett-Packard 524 B Frequency Counter. The magnetic field is measured using the same counter and a Numar Precision Gaussmeter. The field is modulated (usually at 80 cps) using separate coils fastened to the pole faces. A lock-in amplifier and detector at the modulation frequency are employed when recording the signal.

### SPECTRUM EXCLUSIVE OF HYPERFINE STRUCTURE

At 20.4°K the Ni<sup>-</sup> spectrum consists of six main lines having anisotropic  $g$  values. From the symmetry of the

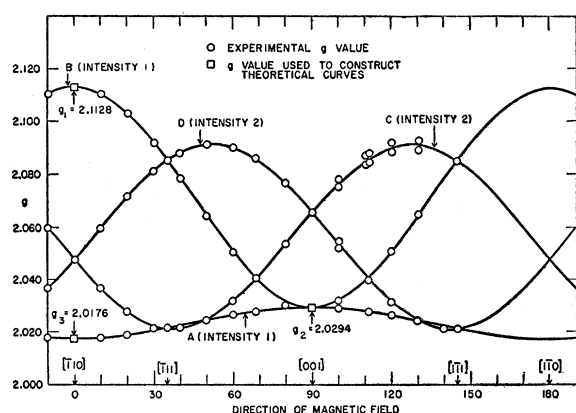


Fig. 2.  $g$  values for the main lines in the Ni<sup>-</sup> spectrum for the dc magnetic field in the plane perpendicular to the  $[110]$  direction.

spectrum and the equal intensities of the lines it is concluded that each nickel site shows only one resonant transition (effective spin  $\frac{1}{2}$ ), but there are six geometrically nonequivalent nickel sites distributed with equal probability throughout the crystal.

The model we have adopted to explain this behavior is depicted in Fig. 1. The nickel impurity occupies a substitutional site in the germanium lattice. The configuration of the Ni<sup>-</sup> ion is not known; however, it may be  $3d^8$  with a bound hole in the valence shell. The spin of the  $d$  shell would then be one, that of the valence shell one-half, and the two could together give the observed spin one-half. The bound hole would make the ground state wave function of the Ni<sup>-</sup> ion orbitally degenerate, and the ion would be expected to undergo a Jahn-Teller distortion to remove this degeneracy. A Jahn-Teller distortion occurring with equal probability along any one of the  $(\pm)$  directions corresponding to the three cubic axes accounts for the observed number

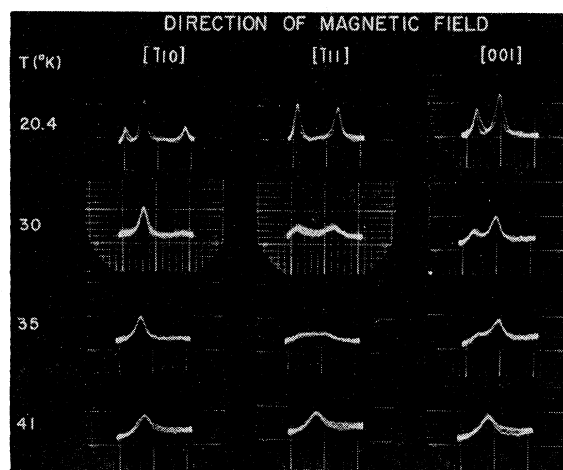


Fig. 3. Photographs of an oscilloscope display of the Ni<sup>-</sup> spectrum as seen in absorption, showing the broadening and merging of the lines as the temperature is raised above 20.4°K.

of lines and the principal axes of the spectrum. One finds that the  $g$  value for any one line is given by the formula

$$g = (g_1^2 \cos^2 \theta_1 + g_2^2 \cos^2 \theta_2 + g_3^2 \cos^2 \theta_3)^{\frac{1}{2}}, \quad (1)$$

where the principal axes of the  $g$ -tensor are the cubic axis along which the distortion takes place and two mutually perpendicular  $[110]$  axes (see Fig. 1 for notation). Since there are six different orientations for the  $g$  ellipsoid, one observes a six-line spectrum.

The spectrum was examined in crystals having a  $[110]$  axis vertical with the dc magnetic field in the horizontal plane. With this arrangement one sees at most four lines of intensities 1:1:2:2, since two pairs of lines always coincide (see Fig. 2). The principal values of the  $g$  tensor are indicated in the figure. The solid curves are the theoretical  $g$  values obtained by substituting  $g_1$ ,  $g_2$ , and  $g_3$  into Eq. (1).

At angles near 120° line C appears as a closely spaced doublet; the splitting is due to a slight misorientation of the crystal ( $[110]$  axis  $\sim 2^\circ$  from the vertical as defined by the magnet).

### TEMPERATURE DEPENDENCE OF THE MAIN SPECTRUM

Figure 3 shows the spectrum observed for three simple directions of magnetic field, the  $[110]$ , the  $[111]$ , and the  $[001]$ , as a function of temperature. At 20.4°K the lines have a full width between maxima on the absorption derivative of 4.2 gauss and the over-all spread of the spectrum is of order 200 gauss. As the temperature is raised the lines broaden and then merge. After merging the resultant (isotropic) line narrows (minimum width  $\sim 28$  gauss) and then widens above 50°K.

The Jahn-Teller distortion is frozen in at sufficiently low temperatures, but reorients with increasing frequency as the temperature is raised. As the frequency of reorientation approaches the low-temperature line

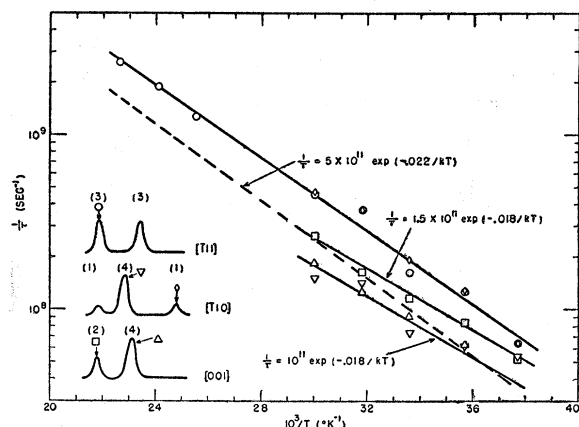


FIG. 4. Correlation time for reorientation of the Jahn-Teller distortion as calculated from line broadening for various lines in the  $\text{Ni}^{2+}$  spectrum. The dashed line is an estimate to  $1/\tau$  for reorientation by inversion only (see text). The numbers in parentheses above the lines are their relative intensities.

width, the lines broaden; as it approaches the over-all splitting between lines, the individual lines merge. If no other broadening mechanism entered, one would expect the width of the single resultant line to approach, at high temperatures, a width no greater than that of the individual lines at very low temperatures.

The widths of a number of lines were measured as a function of temperature. The lines are designated by their relative intensities, namely 1, 2, 3, or 4 according to whether they represent a single one of the six lines seen for arbitrary magnetic field direction or the superposition of 2, 3, or 4 of these lines. The results were analyzed assuming that the effects of motion on line width could be represented by an exponential correlation function for the persistence of a given orientation. For the temperature region where the individual lines were broadening, the correlation time was estimated from calculations<sup>8</sup> of the motional broadening of an originally Gaussian line to a Lorentzian shape. For the two equally intense lines in the  $[\bar{1}11]$  direction (see Fig. 4) the correlation time in the temperature region where the single resultant line is narrowing was calculated using a formula derived from results of Gutowsky *et al.*<sup>9</sup> The formula assumes a Lorentzian line shape; it was used only during the initial stages of narrowing when the line shape is Lorentzian to a good approximation.

The inverse of the correlation time calculated for various lines is shown in Fig. 4. It is not surprising that the inverse correlation times and their temperature dependences differ for different lines. Any reorientation of a site corresponding to a line of unit intensity will

<sup>8</sup> G. D. Watkins has kindly furnished us with the results of such a calculation.

<sup>9</sup> Gutowsky, McCall, and Slichter [*J. Chem. Phys.* **21**, 279 (1953), Eq. (41)]. Experimentally, one-half of the peak-to-peak derivative width was measured at various temperatures. This frequency difference was assumed equal to the value of  $\Delta\omega$  at which  $\partial^2 \text{Re}(\bar{G})/\partial(\Delta\omega)^2 = 0$ . To obtain a formula for  $\tau^{-1}$  in closed form, it was assumed that  $\tau/T_2 \ll 1$ .

transform the site into one having a different  $g$  value. Some reorientations of a site contributing to a line of greater than unit intensity will transform it into a site having the same  $g$  value, and hence are less effective in line broadening.<sup>10</sup> Moreover there are two types of reorientation for the Jahn-Teller distortion, inversion, and rotation. For example, a distortion in the  $[001]$  direction can reorient by inversion to the  $[00\bar{1}]$  direction and by rotation to the  $[100]$ ,  $[\bar{1}00]$ ,  $[010]$ , and  $[0\bar{1}0]$  directions.

The line of intensity one broadens rapidly and follows the uppermost solid line in Fig. 4. The lines of intensity four, which are changed in  $g$  value by two of the four rotations, and not by inversion, broaden least rapidly and follow the lowest solid line in Fig. 4. One notes that the lines of intensity three for the magnetic field in the  $[\bar{1}11]$  direction broaden about as rapidly as the line of intensity one. Sites corresponding to these lines are transformed in  $g$  value by inversion and by two of the rotations. Moreover the line of intensity two in the  $[001]$  direction (changed in  $g$  value by all rotations but not by inversion) broadens almost as slowly as the lines of intensity four.

One may see from Fig. 4 that the data for spectral lines representing sites which change  $g$  value only by rotations can be fitted reasonably well by straight lines. This is evidence that one is dealing with a thermally activated motion. The activation energy shown by the straight lines (0.018 eV) is considered an estimate to the energy barrier to rotation. To obtain an estimate of the energy barrier to inversion, the contribution to  $1/\tau$  from reorientation by rotation was subtracted from the data representing broadening by both inversion and rotation. The dashed line of Fig. 4, showing an activation energy of 0.022 eV, resulted. This energy is also an estimate of the Jahn-Teller energy. Despite the somewhat higher energy barrier, reorientation by inversion competes with reorientation by rotation between 20°K and 40°K because of a higher frequency factor (see Fig. 4). The near equality of barrier heights is not understood.<sup>11</sup>

### $\text{Ge}^{73}$ HYPERFINE STRUCTURE

One might expect hyperfine interaction of the nickel center with  $\text{Ge}^{73}$  (nuclear spin  $I=9/2$ ) occupying the nearest neighbor sites (see Fig. 1). Since there are four such sites one anticipates four sets of ten hyperfine lines

<sup>10</sup> Reorientations which leave the  $g$  value unchanged may contribute to line broadening because of phase accumulation during the reorientation. Competing with this, hyperfine interactions contributing to line width could be partially averaged out by the reorientation.

<sup>11</sup> E. O. Kane of this laboratory calculated the Jahn-Teller energy assuming a hole in a  $j=3/2$  state localized on the Ni atom and ignoring the  $d$  shell. The energy was assumed to be a parabolic function of normal coordinate about the symmetric site excluding the energy from the bound hole. An energy term linear in the normal coordinate was added, representing the Jahn-Teller energy of the hole. Although this simplified model correctly predicted a  $[100]$  distortion as the minimum energy position, it indicated that the energy barrier to inversion was nine times that to rotation.

associated with each main line for arbitrary direction of the magnetic field relative to the crystalline axes. However, the Jahn-Teller distortion moves the nickel atom closer to two of the four nearest neighbors and farther away from the other two. Only two sets of ten well-resolved hyperfine lines are observed; these are attributed to a  $\text{Ge}^{73}$  isotope in either of the two closer positions. Figure 5 shows the hyperfine structure associated with a particular line for the magnetic field in the  $[\bar{1}10]$  direction. For this direction of magnetic field the two sets of ten well-resolved hyperfine lines coincide. Four of these lines are clearly resolved in Fig. 5. An indication of the fifth line is seen at the position where it would be expected, based on the equal spacing of these lines. There remains an extra line between (4) and (5), which is attributed to interaction with  $\text{Ge}^{73}$  in either of the two farther nearest neighbor positions. Presumably it represents the outermost hyperfine line. Assuming ten equally spaced lines (as is found for the resolved hyperfine structure), the splitting between adjacent lines would be  $\sim 4$  gauss. Since the peak-to-peak derivative width is also  $\sim 4$  gauss, the inner lines would tend to cancel on a derivative display of the absorption, which explains why they are not observed.

The expected intensity for a given hyperfine line relative to that of the main line can be calculated on the basis of the known abundance of the  $\text{Ge}^{73}$  isotope (7.7%). The probability of obtaining the main line is the probability  $(1-p)^4$ , where  $p=0.077$ , that none of the nearest neighbors is  $\text{Ge}^{73}$ . The probability of obtaining a given hyperfine line is the probability  $p(1-p)^3$  that a given one of the nearest neighbors is  $\text{Ge}^{73}$  while the others are not, times the probability 0.1 of encountering a given magnetic quantum number  $m_I$ . Thus the relative intensity of a given hyperfine line is predicted to be  $0.1p(1-p)^3/(1-p)^4=0.0084$ . Within 10% this is the relative intensity observed. The observation of ten lines in a set ( $2I+1=10$ ) and the  $[\bar{1}11]$  principal axis for the

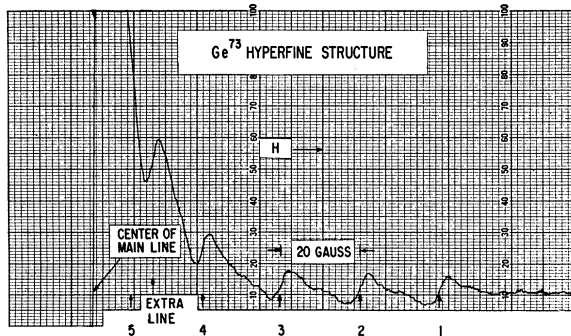


FIG. 5. Absorption derivative on the high-field side of the highest field line (line A) for the magnetic field in a  $[\bar{1}10]$  direction. The lines marked 1-5 are attributed to hyperfine interaction with  $\text{Ge}^{73}$  in either of the two nearest neighbor positions toward which the Ni atom moves in the Jahn-Teller distortion. The extra line is attributed to hyperfine interaction with  $\text{Ge}^{73}$  in either of the two farther nearest neighbor positions.

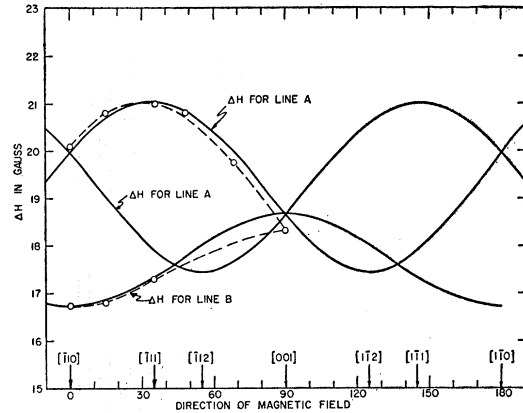


FIG. 6. The splitting  $\Delta H$  between adjacent hyperfine lines due to interaction of the Ni site with  $\text{Ge}^{73}$  in either of the closer two of the four nearest neighbor positions.

resolved hyperfine interaction further confirm the view that one is seeing hyperfine interaction with nearest neighbor  $\text{Ge}^{73}$  atoms.

In the absence of resolved hyperfine interaction with  $\text{Ge}^{73}$ , one could not decide whether the assignment of  $g$  values in Fig. 1 is correct, or whether  $g_1$  and  $g_2$  should be interchanged. However, assuming that the resolved hyperfine structure is due to  $\text{Ge}^{73}$  in the nearest neighbor positions toward which the nickel atom moves, one can assign  $g$  values uniquely. For line B (see Fig. 2) the two sets of resolved lines always coincide; hence line B corresponds to the Jahn-Teller distortion depicted in Fig. 1, and the  $g$  values in the three principal directions are as given in that figure.

The resolved hyperfine interaction with  $\text{Ge}^{73}$  is unusual in that the principal axes describing the interaction differ from those of the  $g$  tensor. Since the interaction represents a small perturbation with respect to the external field, a theoretical expression<sup>12</sup> for the splitting  $\Delta H$  between adjacent hyperfine lines is readily derived. The electron spin  $S$  is quantized along the direction  $\mathbf{g} \cdot \mathbf{H}$ , and the nuclear spin  $I$  of the  $\text{Ge}^{73}$  along the direction  $\mathbf{H} \cdot \mathbf{g} \cdot \mathbf{T}$ , where  $\mathbf{T}$  is the hyperfine interaction tensor.  $\mathbf{T}$  is assumed to have principal values  $T_{11}$  along the Ni- $\text{Ge}^{73}$  direction and  $T_{\perp}$  for any direction perpendicular to that axis. To solve the problem to first order, one may transform  $\mathbf{H} \cdot \mathbf{g}$  to the principal-axis system of  $\mathbf{T}$ . In the case of line A the correct transformation is a rotation of the coordinate axes by an angle  $\alpha$  (equal to  $\pm 54^\circ 44'$ ) about the  $[\bar{1}10]$  direction, while for line B the same rotation should be performed about the  $[\bar{1}10]$  direction.

For the magnetic field in a (110) plane making an angle  $\varphi$  with the  $[\bar{1}10]$  axis, one finds for line A,

$$\Delta H = [\Delta H_{11}^2 (\cos \alpha \cos \varphi - \sin \alpha \sin \varphi)^2 + (g_{\perp} g_0^{-1} \Delta H_{\perp})^2 (\cos \alpha \cos \varphi - \sin \alpha \sin \varphi)^2]^{\frac{1}{2}}, \quad (2)$$

where the small anisotropy in the  $g$  value for line A has

<sup>12</sup> We are indebted to E. O. Kane for examining this problem.

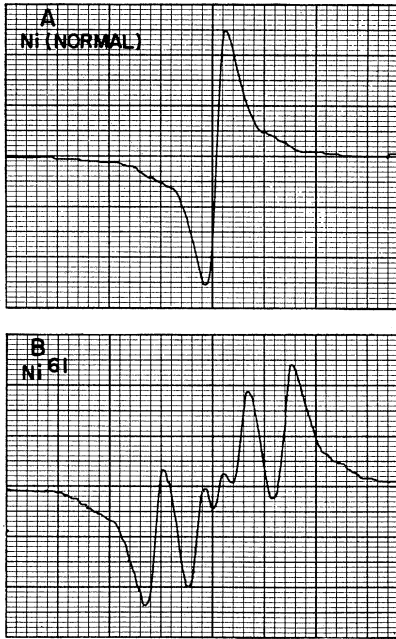


FIG. 7. The absorption derivative at 20.4°K for line *B* (see Fig. 2) in the  $[\bar{1}10]$  direction in a sample *A* doped with nickel of normal isotopic abundance and in a sample *B* doped with nickel enriched to contain 83%  $\text{Ni}^{61}$ . The nickel content of the two samples is about the same, but the gain of the spectrometer was about five times greater for recording *B*.

been neglected ( $g$  taken as  $g_0=2.02$ ),  $\Delta H_{11}$  is the maximum splitting for line *A*, and  $\Delta H_1$  is the minimum splitting for line *B*.

Similarly, for line *B*,

$$\Delta H = g^{-2} [(g_0 \Delta H_{11})^2 (g_2 \cos \alpha \sin \varphi)^2 + (g_1 \Delta H_1)^2 (g_1^2 \cos^2 \varphi + g_2^2 \sin^2 \alpha \sin^2 \varphi)]^{1/2}. \quad (3)$$

Measured hyperfine splittings for lines *A* and *B* are shown in Fig. 6. Additional experimental values were difficult to determine because of overlapping of hyperfine lines with each other and with the main lines of the nickel spectrum, but were consistent with the data shown. One notes that the experimental points lie on slightly different curves than the solid lines which are plots of Eq. (2) and Eq. (3). Such a displacement would be expected if the nickel atom moved a finite distance in the Jahn-Teller distortion, since the motion would distort the angles between the nickel and the nearest neighbor germanium atoms. A motion of 0.2 Å, which corresponds to a change in bond angle of about 4°, would bring the experimental and theoretical curves closer to coincidence.

The resolved hyperfine interaction, attributed to  $\text{Ge}^{73}$  in either of the two closer nearest neighbor positions, has principal values  $T_{11}=19.8 \times 10^{-4} \text{ cm}^{-1}$  and  $T_1=16.5 \times 10^{-4} \text{ cm}^{-1}$ . It is a factor of 4 or 5 stronger than that with  $\text{Ge}^{73}$  in either of the two farther nearest neighbor positions.

### $\text{Ni}^{61}$ HYPERFINE STRUCTURE

In samples prepared with nickel enriched in  $\text{Ni}^{61}$ , the main lines of the nickel spectrum show additional hyperfine structure.<sup>5</sup> Figure 7 shows line *B* for the  $[\bar{1}10]$  direction in a sample *A* containing nickel of normal isotopic abundance and in a sample *B* enriched to contain 83%  $\text{Ni}^{61}$ . In sample *B* one sees five lines. The small center line has a  $g$  value identical to that of sample *A*, and arises from the 17% abundant Ni isotopes of spin zero. The other four lines correspond to the four possible orientations of the  $\text{Ni}^{61}$  nucleus and indicate a spin of  $\frac{3}{2}$  for that isotope. To our knowledge this is the first experimental determination of the spin of  $\text{Ni}^{61}$ .

The  $\text{Ni}^{61}$  hyperfine structure is anisotropic, but has, as expected, the same principal axes as the  $g$  tensor. Referring to the notation of Fig. 1, the principal values  $A_1$ ,  $A_2$ , and  $A_3$  for the hyperfine interaction with  $\text{Ni}^{61}$  are 10.3,  $\leq 1.6$  and 12.2, respectively, in units of  $10^{-4} \text{ cm}^{-1}$ .

### SUMMARY

$\text{Ni}^-$  in germanium shows an effective spin  $S=\frac{1}{2}$  and an anisotropic  $g$  tensor at 20.4°K and below. The anisotropy is attributed to a Jahn-Teller distortion in a cubic direction, giving, for example, as the principal axes of the  $g$  tensor the  $[001]$  direction of the distortion, the  $[\bar{1}10]$  direction from one to the other of the nearest neighbor germanium atoms toward which the nickel atom moves, and the  $[\bar{1}10]$  direction at right angles to the two previous directions. The principal values of the  $g$  tensor are  $g_2=2.0294$ ,  $g_3=2.0176$ , and  $g_1=2.1128$ , respectively. The  $\text{Ni}^{61}$  hyperfine interaction has the same principal axes, and principal values  $A_2 \leq 1.6$ ,  $A_3=12.2$ , and  $A_1=10.3$ , respectively, in units of  $10^{-4} \text{ cm}^{-1}$ . Resolved hyperfine interaction is observed with  $\text{Ge}^{73}$  in either of the two nearest neighbor positions toward which the nickel atom moves. The hyperfine interaction is a maximum when the magnetic field points in the Ni- $\text{Ge}^{73}$  direction ( $T_{11}=19.8 \times 10^{-4} \text{ cm}^{-1}$ ) and a minimum for the magnetic field at right angles to this axis ( $T_1=16.5 \times 10^{-4} \text{ cm}^{-1}$ ).

As the temperature is raised above 20.4°K the Jahn-Teller distortion, which was frozen in at low temperatures, reorients with increasing rapidity, and the lines broaden and eventually merge. Different lines broaden at different rates since some reorientations leave the  $g$  value unchanged (for particular directions of the external field) and since two types of reorientation, inversion and rotation, must be considered. The barrier to inversion is about 0.02 eV.

### ACKNOWLEDGMENTS

The authors thank E. O. Kane and G. D. Watkins for many helpful discussions and R. L. Watters for assistance with the circuitry. The samples were furnished by W. W. Tyler. C. R. Trzaskos assisted with the measurements.

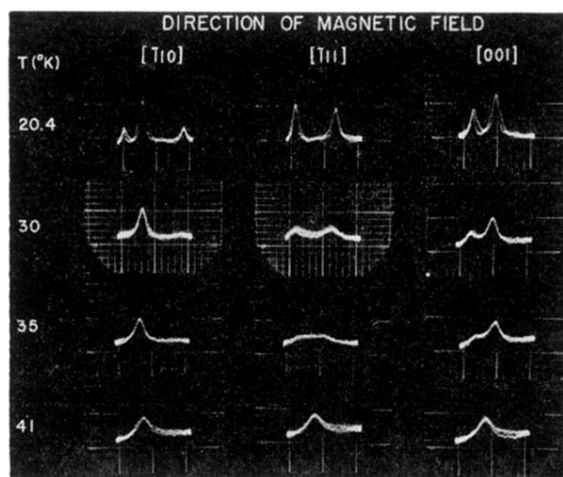


FIG. 3. Photographs of an oscilloscope display of the Ni<sup>2+</sup> spectrum as seen in absorption, showing the broadening and merging of the lines as the temperature is raised above 20.4°K.